Endothelial C-type natriuretic peptide maintains vascular homeostasis

Amie J. Moyes,[1] Rayomand S. Khambata,[1] Inmaculada Villar,[1] Kristen J. Bubb,[1] Reshma S. Baliga,[1] Natalie G. Lumsden,[1] Fang Xiao,[1] Paul J. Gane,[2] Anne-Sophie Rebstock,[2] Roberta J. Worthington,[2] Michela I. Simone,[2] Filipa Mota,[2] Fernando Rivilla,[3] Susana Vallejo,[4] Concepción Peiró,[4] Carlos F. Sánchez Ferrer,[4] Snezana Djordjevic,[5] Mark J. Caulfield,[1] Raymond J. MacAllister,[6] David L. Selwood,[2] Amrita Ahluwalia,[1] and Adrian J. Hobbs[1]

[1]William Harvey Research Institute, Barts and The London School of Medicine and Dentistry, Queen Mary University of London, London, United Kingdom. [2]Wolfson Institute for Biomedical Research, University College London, London, United Kingdom. [3]División de Cirugía Pediátrica, Hospital Universitario Ramón y Cajal, Madrid, Spain. [4]Departamento de Farmacologia, Facultad de Medicina, Universidad Autonoma de Madrid, Madrid, Spain. [5]Structural and Molecular Biology and [6]Clinical Pharmacology, University College London, London, United Kingdom.

The endothelium plays a fundamental role in maintaining vascular homeostasis by releasing factors that regulate local blood flow, systemic blood pressure, and the reactivity of leukocytes and platelets. Accordingly, endothelial dysfunction underpins many cardiovascular diseases, including hypertension, myocardial infarction, and stroke. Herein, we evaluated mice with endothelial-specific deletion of *Nppc*, which encodes C-type natriuretic peptide (CNP), and determined that this mediator is essential for multiple aspects of vascular regulation. Specifically, disruption of CNP leads to endothelial dysfunction, hypertension, atherogenesis, and aneurysm. Moreover, we identified natriuretic peptide receptor–C (NPR-C) as the cognate receptor that primarily underlies CNP-dependent vasoprotective functions and developed small-molecule NPR-C agonists to target this pathway. Administration of NPR-C agonists promotes a vasorelaxation of isolated resistance arteries and a reduction in blood pressure in wild-type animals that is diminished in mice lacking NPR-C. This work provides a mechanistic explanation for genome-wide association studies that have linked the NPR-C (*Npr3*) locus with hypertension by demonstrating the importance of CNP/NPR-C signaling in preserving vascular homoeostasis. Furthermore, these results suggest that the CNP/NPR-C pathway has potential as a disease-modifying therapeutic target for cardiovascular disorders.

Introduction

The vascular endothelium releases an array of vasorelaxant mediators that not only influence the tone and growth of the underlying smooth muscle, but also regulate the reactivity of leukocytes and platelets (1, 2). Endothelial dysfunction, a reduced capacity of the endothelium to release these cytoprotective signaling molecules, is a major precipitating factor in cardiovascular disease (e.g., hypertension, myocardial infarction, and stroke) that accounts for the greatest number of deaths in Western societies (3, 4). Perhaps the most important endothelium-derived paracrine mediators are nitric oxide (NO) and prostacyclin (PGI_2), each well established as playing a multifaceted role in vascular homeostasis (1, 5, 6). In many arteries, however, particularly those in the resistance vasculature, substantial endothelium-dependent dilatation persists following inhibition of NO and PGI_2 synthesis. This residual non-NO, nonprostanoid vasorelaxant activity is attributed to endothelium-derived hyperpolarization (EDH) and is established as playing a fundamental role in regulating resistance artery tone and systemic blood pressure (7). The mechanism or mechanisms underpinning EDH remain controversial, but it is believed to be more prominent in females than males and may contribute to the cardioprotective phenotype experienced by premenopausal women when compared with age-matched male counterparts (8–10).

In concert with local endothelial production of NO and PGI_2, cardiac-derived atrial and brain natriuretic peptides (ANP and BNP) possess well-defined endocrine functions in maintaining electrolyte balance, blood volume, vascular tone, and cardiac integrity (11, 12). The third member of this peptide family, C-type natriuretic peptide (CNP), has clearly delineated roles in bone growth(13, 14); there is, however, a paucity of evidence supporting a physiological role for this peptide in cardiovascular homeostasis. Yet the intriguing pharmacodynamic profile of exogenous CNP in vascular cells and tissues in vitro (15, 16) coupled with the significant expression of CNP in endothelial cells (17, 18) intimates that it possesses an ideal functional capacity and tissue localization to influence vascular dynamics.

Herein, we have developed and characterized a mouse model with endothelial-specific deletion of CNP to delineate a role for the peptide in vascular homeostasis. Utilizing this unique tool, we reveal that CNP is a major component of the non-NO, nonprostanoid component of endothelium-dependent relaxation in the resistance vasculature (i.e., EDH) and that loss of CNP signaling results in vascular dysfunction, hypertension, atherogenesis, and aneurysm. Moreover, we identify activation of natriuretic peptide receptor–C (NPR-C) as the principal route via which CNP regulates vascular tone and integrity and describe the development of small-molecule

Conflict of interest: The authors have declared that no conflict of interest exists.
Submitted: November 14, 2013; **Accepted:** June 19, 2014.
Reference information: *J Clin Invest*. 2014;124(9):4039–4051. doi:10.1172/JCI74281.

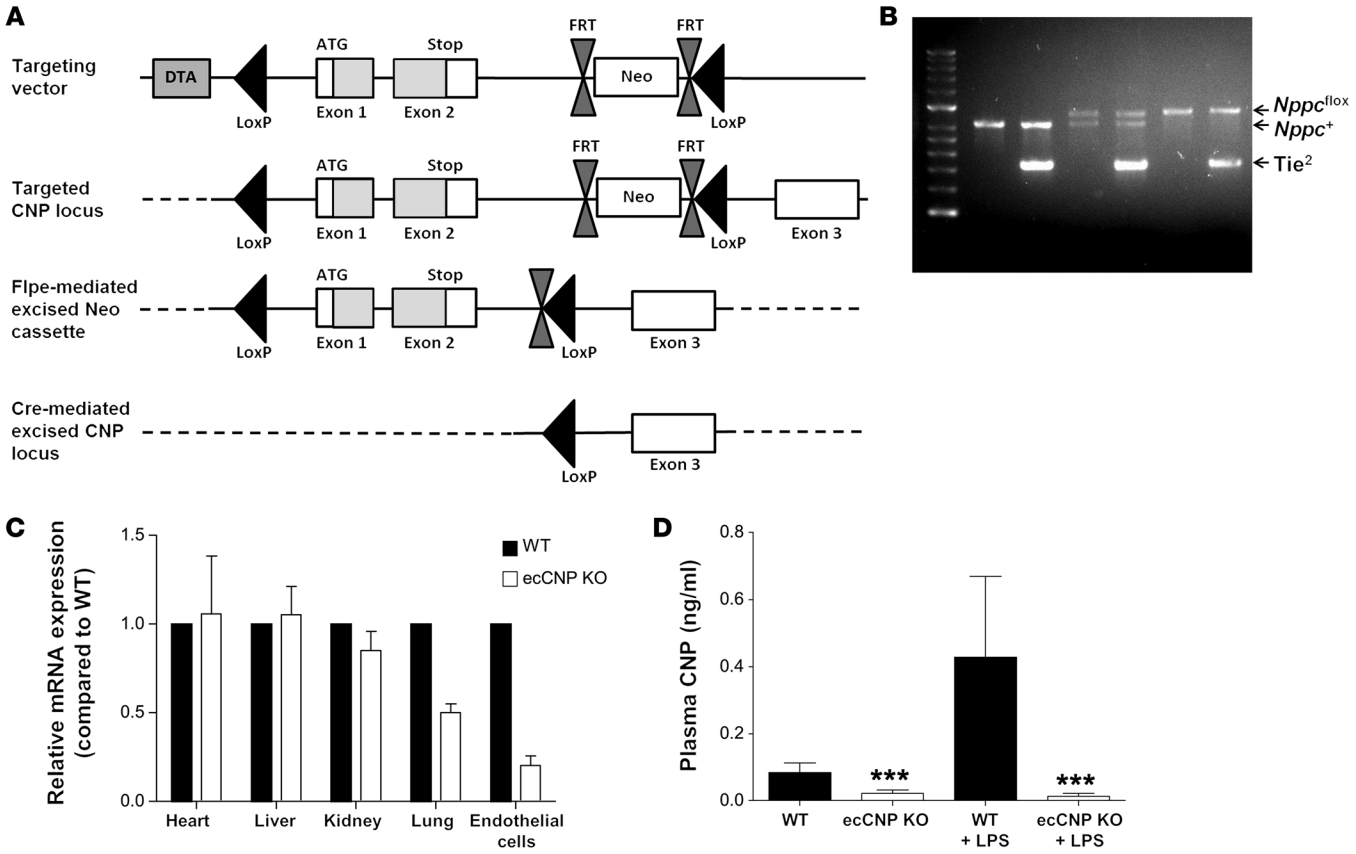

Figure 1. Development and characterization of an endothelium-specific CNP knockout mouse. Cell-specific deletion of the *CNP* gene was achieved by flanking exons 1 and 2 of the *CNP* (*Nppc*) gene with LoxP sites (**A**). Flippase recognition target (FRT) sites were used to permit efficient removal of the neomycin cassette by breeding chimeric mice with ubiquitous *Flpe*-expressing animals, resulting in the generation of $Nppc^{+/fl}$ offspring. $Nppc^{fl/fl}$ animals were then crossed with a mouse in which expression of Cre recombinase is driven by an endothelial-specific promoter/enhancer associated with the angiopoietin Tie^2 receptor. Heterozygous animals at the *Nppc* locus that expressed the Tie^2 transgene (Tie^2-*Cre* $Nppc^{+/fl}$) were used as breeding pairs to generate ecCNP KO and corresponding WT (Tie^2-*Cre* $Nppc^{+/+}$) littermate controls. Analysis of the DNA from these animals confirmed generation of the 6 possible genotypes (**B**). qPCR analysis of *CNP* mRNA from different tissues established that the *CNP* gene had been deleted selectively from vascular endothelial cells (**C**). Measurement of plasma CNP concentrations under basal conditions and following administration of LPS (12.5 mg/kg; i.p.; 12 h) confirmed that peptide levels were significantly reduced in ecCNP KO versus WT animals (**D**). Data are represented as the mean ± SEM. $n = 5$. $^{***}P < 0.001$, significantly different from corresponding WT littermates.

NPR-C agonists that recapitulate the vasoprotective actions of this peptide. These data establish the importance of CNP/NPR-C signaling in the physiological control of vascular dynamics and the druggable nature of this pathway for cardiovascular disease.

Results

Development and characterization of an endothelium-specific CNP knockout mouse. We abrogated CNP expression in endothelial cells via a tissue-specific excision of the *Nppc* gene using Cre-Lox technology (ref. 19 and Figure 1, A and B). Expression of *CNP* mRNA was significantly reduced (~80%) in microvascular endothelial cells isolated from Tie^2-*Cre* $Nppc^{fl/fl}$ mice (hereafter referred to as endothelium-specific CNP knockout [ecCNP KO] mice) compared with WT littermates (Figure 1C). In contrast, *CNP* mRNA expression was equivalent in all other tissues examined from WT and KO animals, with the exception of the lungs in which lower levels are probably indicative of loss of endothelial CNP from this organ. *CNP* mRNA was also detected at commensurate levels in the leukocyte subpopulations from WT and KO mice (indeed, if anything, *CNP* mRNA levels were increased in the neutrophil population from ecCNP KO animals), confirming that Tie^2-driven Cre expression was not deleting CNP from hematopoietic cells (Table 1). Under both basal conditions, and following administration of the inflammogen LPS (a potent trigger for CNP release from endothelial cells, ref. 17), plasma CNP concentrations were significantly higher in WT compared with KO mice (Figure 1D). In concert, these data confirm efficient, exclusive removal of the *Nppc* gene from the vascular endothelium.

Table 1. *CNP* mRNA expression in the leukocyte population of ecCNP KO animals compared with WT littermates

	Neutrophils	Monocytes	T cells	B cells
Relative *CNP* mRNA expression (WT = 1)	7.13 ± 1.19	2.67 ± 1.61	1.31 ± 0.41	1.80 ± 0.54

$n = 5$.

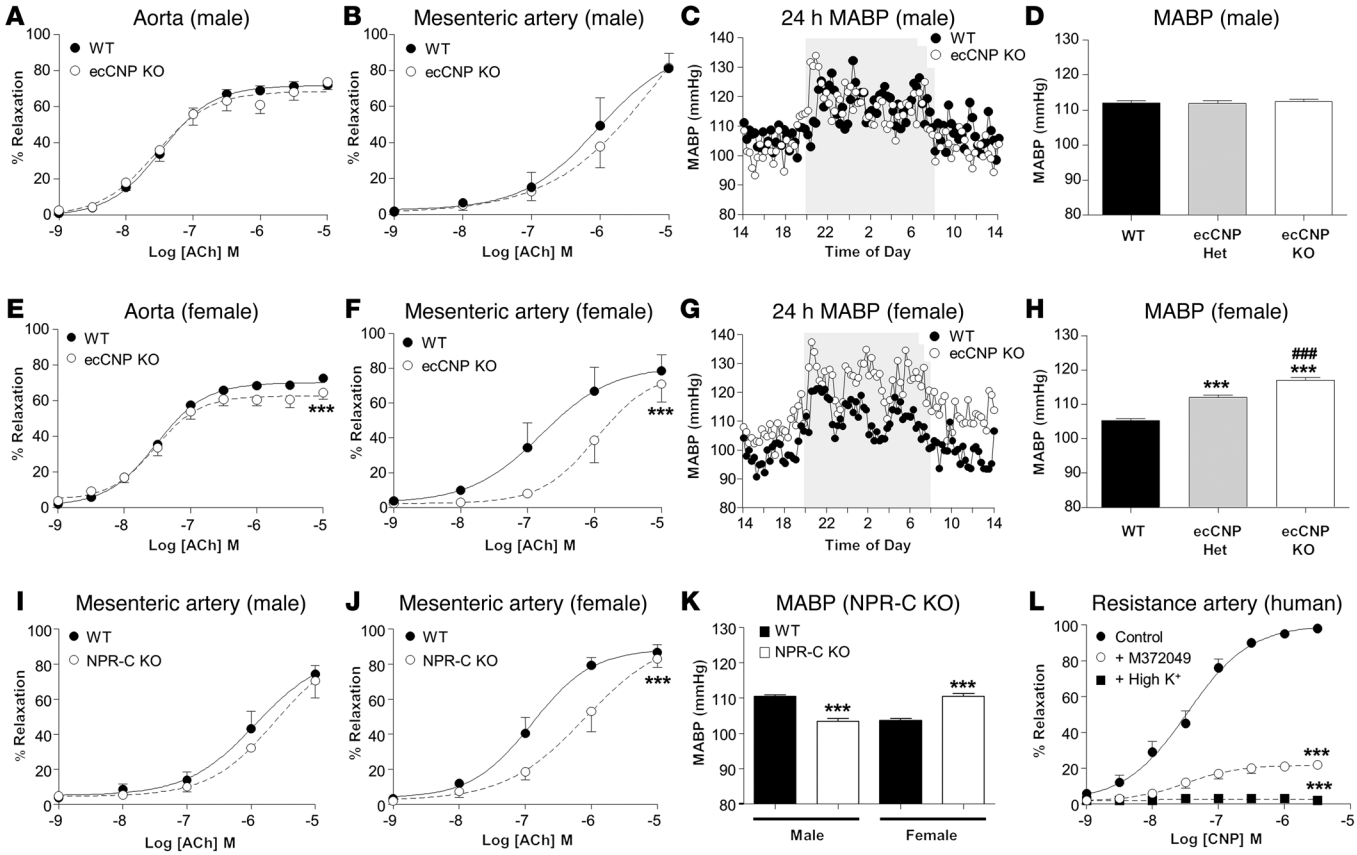

Figure 2. Endothelial dysfunction and hypertension in ecCNP KO mice. Endothelium-dependent relaxation to ACh in isolated aorta and mesenteric artery of male ecCNP KO animals was unaltered in comparison with that of littermate controls (**A** and **B**). In contrast, there was a small reduction in maximal ACh relaxation in the aorta (**E**) and significant decrease in potency to ACh in the mesenteric arteries (**F**) of female ecCNP KO animals. MABP of male (**C** and **D**) and female (**G** and **H**) WT and ecCNP KO animals paralleled the in vitro vascular reactivity with a hypertensive phenotype only apparent in females; heterozygous ecCNP animals exhibited an intermediate phenotype (**H**). An analogous endothelial dysfunction (**J**) and hypertensive phenotype (**K**) was apparent in female NPR-C KO animals, whereas male NPR-C KO mice maintained normal endothelial function (**I**) and exhibited a mild hypotensive phenotype (**K**). CNP relaxed human mesenteric resistance arteries in a concentration-dependent manner and was sensitive to the NPR-C antagonist M372049 and high $[K^+]$ (**L**). Vasorelaxant responses in **B**, **F**, **I**, **J**, and **L** were obtained in the presence of L-NAME and indomethacin. Data are represented as the mean ± SEM. $n = 6$ for isolated vessel studies, $n = 8$ for the in vivo MABP studies. $^{***}P < 0.001$, significantly different from WT littermates; $^{\#\#\#}P < 0.01$, significantly different from heterozygote littermates.

Vascular reactivity in endothelial CNP knockout mice. We compared the in vitro vascular reactivity of conduit (aorta) and resistance (mesenteric) arteries from WT and ecCNP KO mice. Responses to the vasoconstrictors phenylephrine (α_1-adrenoceptor agonist) and U46619 (thromboxane A_2 mimetic) were identical in vessels taken from WT and ecCNP KO animals regardless of sex (Supplemental Figure 1, A–H; supplemental material available online with this article; doi:10.1172/JCI74281DS1). In the aorta, the endothelium-dependent dilator acetylcholine (ACh) produced concentration-dependent relaxations of both WT and ecCNP KO tissues with analogous potency and efficacy, albeit with a small reduction in maximal relaxation in the female ecCNP KO mice (Figure 2, A and E); these data are in accord with previous work establishing that such relaxations are primarily dependent on the release of endothelium-derived NO and PGI_2 (20). In marked contrast, in mesenteric small arteries, there was a significant rightward shift (indicative of decreased potency) in the vasorelaxant concentration-response curve to ACh in female (Figure 2F), but not male (Figure 2B), vessels. This sex-dependent endothelial impairment was apparent whether studies were conducted in the presence (Figure 2, B and F) or absence (Supplemental Figure 1, I and J) of endothelial NO synthase (eNOS) and cyclooxygenase (COX) inhibition (to prevent the production of NO and PGI_2, respectively). These observations establish that endothelium-derived CNP is a key component of EDH. Importantly, the aberrant vascular reactivity in female ecCNP KO mice was due to a loss of endothelial function and not a change in smooth muscle responsiveness, since relaxant responses to exogenous CNP (Supplemental Figure 2K) and the endothelium-independent dilator spermine-NONOate (an NO-donor drug; ref. 21 and Supplemental Table 1) were comparable between WT and ecCNP KO mice.

Impact of endothelial disruption of CNP on blood pressure. Having established a functional endothelial deficit in the resistance vasculature of ecCNP KO mice, we investigated whether this resulted in a hypertensive phenotype in vivo. In female ecCNP KO mice, the mean arterial blood pressure (MABP) was significantly higher than that of WT littermates (Figure 2, G and H), resulting from increases in both systolic (WT: 119.4 ± 0.67 mmHg, ecCNP KO:

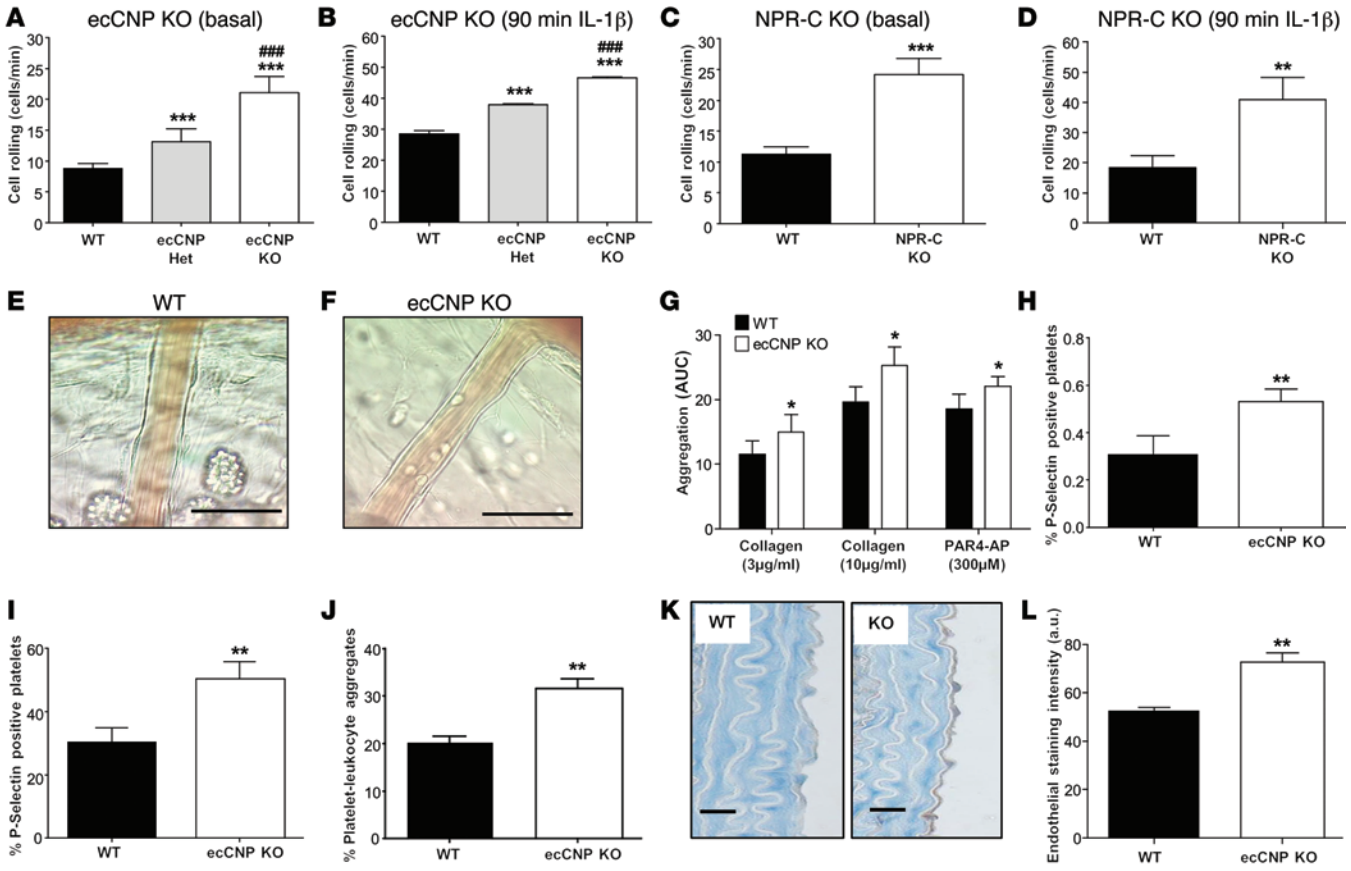

Figure 3. Leukocyte and platelet hyperreactivity in ecCNP KO mice. Basal and IL-1β–stimulated (5 ng/mouse; i.p.) leukocyte rolling was significantly greater in ecCNP KO (**A** and **B**) and NPR-C KO (**C** and **D**) mice compared with WT littermates. Representative images of basal rolling are shown (**E** and **F**). Platelet aggregation in response to collagen (3 μg/ml and 10 μg/ml) and PAR4-AP (300 μM; **G**), basal and PAR4-AP–triggered platelet expression of P-selectin (**H** and **I**), and the level of circulating platelet-leukocyte aggregates (**J**) was greater in ecCNP KO mice compared with WT littermates, implying that CNP regulates platelet function (and leukocyte recruitment) via inhibition of P-selectin expression. Endothelial P-selectin expression was also significantly greater in the aorta of ecCNP KO versus WT mice (**K** and **L**). Data are represented as the mean ± SEM. $n = 10$ for leukocyte studies; $n = 6$ for platelet reactivity and flow cytometry experiments. $^{*}P < 0.05$, $^{**}P < 0.01$, $^{***}P < 0.001$, significantly different from WT littermates; $^{\#\#\#}P < 0.001$, significantly different from heterozygote littermates. Scale bars: 50 μm (**E** and **F**); 20 μm (**K**).

129.1 ± 0.82 mmHg, $P < 0.001$, $n = 8$) and diastolic pressure (WT: 90.2 ± 0.48 mmHg, ecCNP KO: 104.4 ± 0.83 mmHg, $P < 0.001$, $n = 8$). There was no significant difference in heart rate, although heart rate variability (HRV), a risk factor for cardiovascular disease (22), was increased in ecCNP KO animals (Supplemental Table 2). The hypertensive phenotype was evident both day and night, but without any overt effect on the circadian rhythm. Heterozygous animals with one *Nppc* allele deleted (*Tie*^{2}*-Cre Nppc*$^{+/fl}$) exhibited an intermediate blood pressure phenotype (Figure 2H), establishing haploinsufficiency at the *Nppc* locus. The sex disparity in endothelial dysfunction observed in vitro was translated to the physiological setting, since MABP was not significantly raised in males (Figure 2, C and D). Thus, the analogous sex-dependent in vitro vascular dysfunction and raised blood pressure in vivo provide evidence that it is the loss of endothelial function at a local level that underpins the systemic abnormality; more specifically, endothelial CNP deficiency results in impaired vascular homeostasis.

Functional role of NPR-C in maintaining blood pressure. In mammals, the biological activity of CNP is reliant on binding to 1 of 2 cognate receptors: NPR-B, a guanylate cyclase–coupled protein, or NPR-C, a GPCR (23). Our previous work has provided evidence that exogenous CNP mediates vasorelaxation in resistance arteries via NPR-C and activation of a G-protein gated inwardly rectifying potassium channel (GIRK) (24, 25). In order to delineate the receptor that CNP triggers to maintain vascular homeostasis, we examined mesenteric vascular function and blood pressure in *Npr3* KO (NPR-C KO) mice. Here, the loss of responsiveness to ACh observed in ecCNP KO animals was recapitulated (Figure 2, I and J), with endothelial dysfunction observed in vessels from female, but not male, NPR-C KO mice. In accord with this sex difference in vascular function, female NPR-C animals exhibited a hypertensive phenotype whereas male NPR-C KO mice did not (Figure 2K). Indeed, male NPR-C KO animals had a marginally reduced blood pressure, as described previously (26), which corresponds to the conventional clearance function of NPR-C to remove natriuretic peptides from the circulation (26, 27). Further evidence supporting a role for NPR-C as the principal receptor triggered by endothelial CNP to elicit vasodilation and lower MABP was gleaned from experiments using exogenous CNP. The vasorelaxant activity of CNP was blunted in mesenteric vessels from NPR-C KO animals

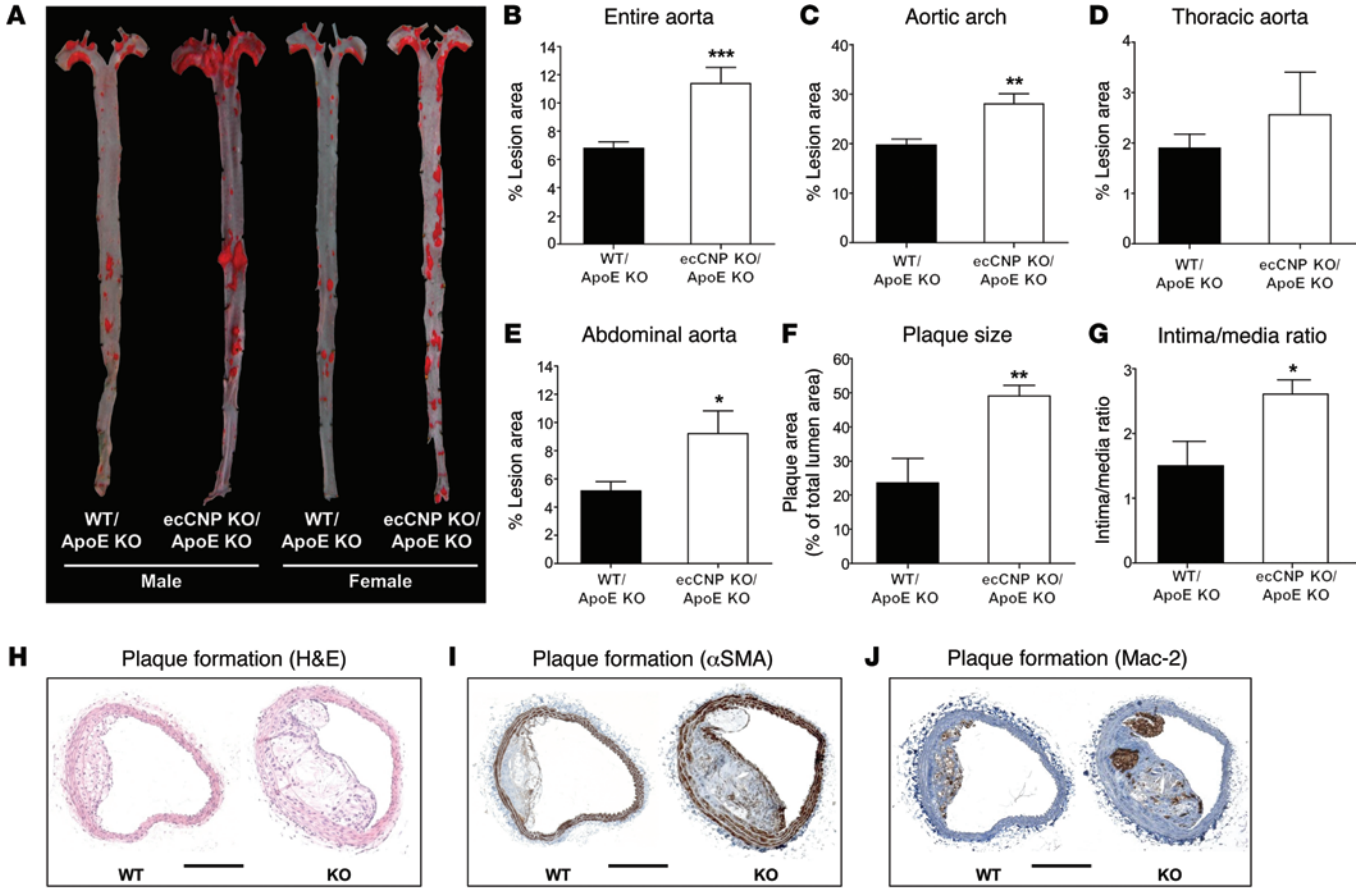

Figure 4. Accelerated atherogenesis in ecCNP KO mice. Atherosclerotic plaque formation was accelerated in the ecCNP/ApoE dKO animals in comparison with WT/ApoE KO. A representative image of oil red O staining of the lesions in the aortic tree is shown (**A**), with quantification of plaque area in the entire aorta (**B**), aortic arch (**C**), thoracic aorta (**D**), and abdominal aorta (**E**). Histological staining of the brachiocephalic arteries from these mice showed a larger plaque size (**F** and **H**), greater intima media thickness ratio (**G** and **I**), and macrophage infiltration (**J**). Data are represented as the mean ± SEM. $n = 18$. $^*P < 0.05$, $^{**}P < 0.01$, $^{***}P < 0.001$, significantly different from WT/ApoE KO littermates. Scale bars: 200 μm (**H**–**J**).

(Supplemental Figure 1K), and in accord, the hypotensive response to CNP in vivo was also diminished in NPR-C KO mice (Figure 6I). Since previous work has demonstrated that NPR-B KO animals are normotensive (28), these observations as a whole provide convincing evidence that, physiologically, NPR-C is the primary receptor triggered by CNP to maintain vascular function and blood pressure. The thesis is supported by the acute vasodilator (29, 30) and hypotensive (31–34) responses to exogenous CNP and the emerging signaling role of G_i-coupled NPR-C in various cell types (35–39).

CNP also produced a concentration-dependent relaxation of human vessels that was abolished in the presence of the selective NPR-C antagonist M372049 (lead compound based on AP-811; gift of C. Veale, AstraZeneca) (25, 40) and following precontraction mediated by high K^+ (which abrogates smooth muscle hyperpolarization; Figure 2L). These data confirm that an NPR-C–triggered hyperpolarization is responsible for the vasorelaxant activity of CNP in human resistance arteries and provide proof-of-concept that the signaling pathway we have identified is functionally important in the human cardiovascular system.

The role of CNP in leukocytes and platelets. Having established CNP as a pivotal physiological regulator of vascular tone and blood pressure, we probed the functional significance of endothelium-derived CNP on leukocyte and platelet reactivity. Leukocyte recruitment is a sequential, multistep process involving rolling, adhesion, and migration of cells orchestrated by a number of adhesion molecules expressed on both leukocytes and endothelial cells and chemokines that direct cells to the site of infection or injury along a concentration gradient (41). In mesenteric postcapillary venules of ecCNP KO, basal leukocyte rolling (an index of leukocyte recruitment) was almost double that observed in WT littermates (Figure 3, A, B, and F; representative observations from WT and ecCNP KO animals, respectively, are shown in Supplemental Videos 1 and 2). These data imply that endothelium-derived CNP maintains a resting antileukocyte influence on the vascular wall. The hyperreactivity of leukocytes in ecCNP KO mice was further illustrated in animals administered the inflammogen IL-1β (Figure 3B). The heterozygous animals displayed an intermediate phenotype in terms of leukocyte rolling under both basal and inflammatory conditions (Figure 3, A and B). There was no significant difference between erythrocyte velocity and wall shear rates in vessels from WT and ecCNP KO animals (Supplemental Table 3), confirming that the changes observed were not the result of alterations in vessel diameter or blood flow. This apparent antiinflammatory role for endothelium-derived CNP was substantiat-

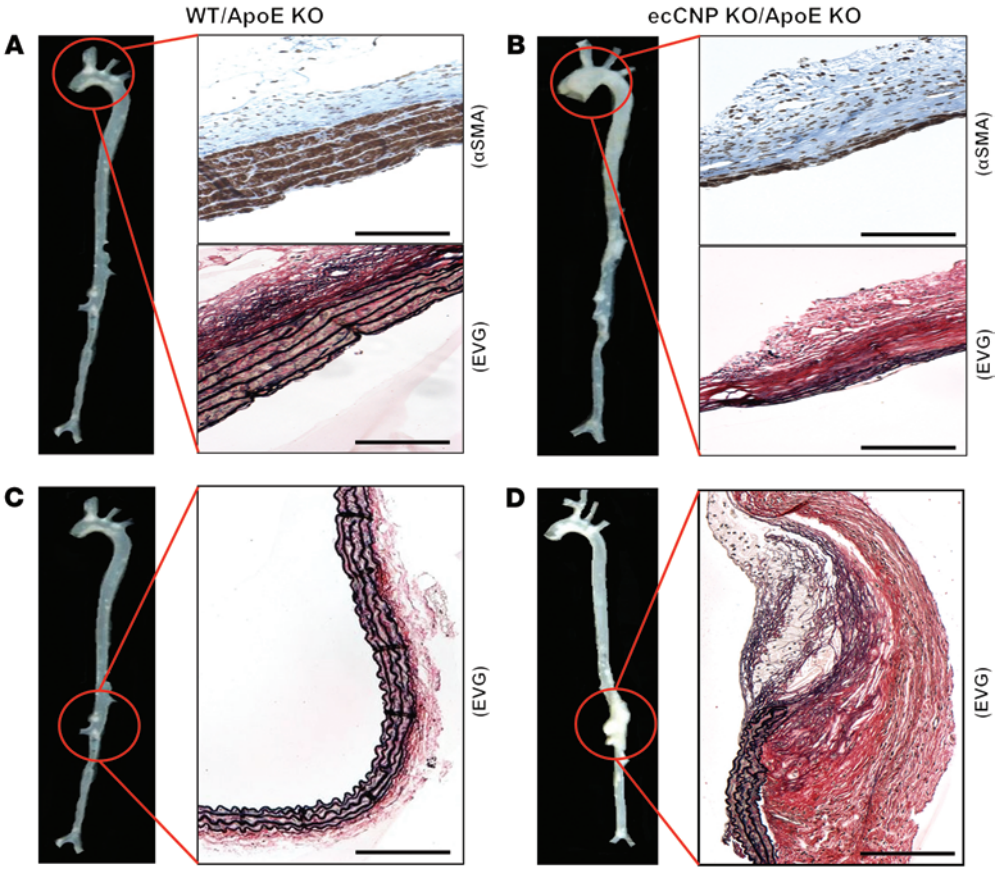

Figure 5. Aneurysm development in ecCNP KO mice. Images of the aneurysms in male ecCNP KO/ApoE KO mice show dilation of the aortic arch (**B**) or abdominal aorta (**D**), loss of vascular smooth muscle and thinning of the vascular wall (**B**), and degradation of elastin (**D**) in comparison with WT/ApoE KO animals (**A** and **C**). Scale bars: 50 μm. Representative of 4/9 male animals. EVG, elastic van Gieson.

ed using a peritonitis model. Following administration of TNF-α, the accumulation of neutrophils and inflammatory macrophages in the peritoneum was significantly greater in ecCNP KO animals versus WT littermates; a similar increase was observed in myeloperoxidase (MPO) activity (an index of neutrophil activation; Supplemental Figure 2). Importantly, in contrast to the blood pressure phenotype, there was no sex difference observed in leukocyte recruitment (data are a composite of observations from male and female mice). Further studies revealed that similar increases in leukocyte rolling were observed in NPR-C KO mice (Figure 3, C and D), suggesting that an identical signal-transduction system that underpins the hypotensive effect of CNP is also responsible for the peptide's antileukocyte activity.

Additional investigation provided strong evidence that endothelium-derived CNP also exerts an antiplatelet influence. In whole blood, we show that platelet aggregation in response to collagen and the thrombin mimetic protease activated receptor-4 activating peptide (PAR4-AP) is exacerbated in ecCNP KO mice (Figure 3G). Akin to leukocyte reactivity, there was no sex difference in this antiplatelet effect of CNP (data are a composite of observations from male and female mice). Flow cytometry was employed to garner insight into the mechanism or mechanisms underpinning the antiplatelet effect of endothelium-derived CNP. These studies illustrated 2 key points. First, platelet P-selectin expression was significantly elevated under basal conditions and following addition of PAR4-AP in ecCNP KO mice compared with WT littermates (Figure 3, H and I). Second, ecCNP KO mice have a significantly greater number of circulating platelet-leukocyte aggregates in comparison with WT animals (Figure 3J). Both are recognized indices of platelet reactivity and cardiovascular inflammation (42, 43) and suggest that endothelium-derived CNP maintains a subtle, yet important dampening of platelet function in vivo. Moreover, a similar increase in P-selectin expression was observed on endothelial cells (Figure 3, K and L). The prominence of P-selectin in leukocyte extravasation and platelet-endothelium/platelet-leukocyte interactions (44) suggests that an NPR-C–driven suppression of P-selectin expression is a common mechanism underpinning the antileukocyte and antiplatelet effects of CNP.

CNP influences atherosclerosis and aneurysm formation. In light of the observation above, we hypothesized that ecCNP KO mice would exhibit increased susceptibility to atheroma formation. To address this, we exploited a well-validated experimental model of atherogenesis, the apolipoprotein E (*Apoe*) KO mouse (45, 46). The development of atherosclerotic plaque in the aorta of ecCNP/ApoE double KO (dKO) mice was significantly accelerated when compared with the corresponding CNP WT/ApoE KO littermates. This manifested as considerably greater plaque area throughout the entire aorta, with the most notable increases in the aortic arch and the suprarenal region of the abdominal aorta (Figure 4, A–E). Furthermore, cross-sectional analysis of the brachiocephalic artery revealed that plaque intrusion into the vessel lumen and the development of a neointimal layer characterized by vascular smooth muscle hyperplasia were significantly greater in the ecCNP/ApoE dKO mice (Figure 4, F–H). This increased plaque burden was also accompanied by an increased infiltration of smooth muscle cells and macrophages into the lesions (Figure 4, I

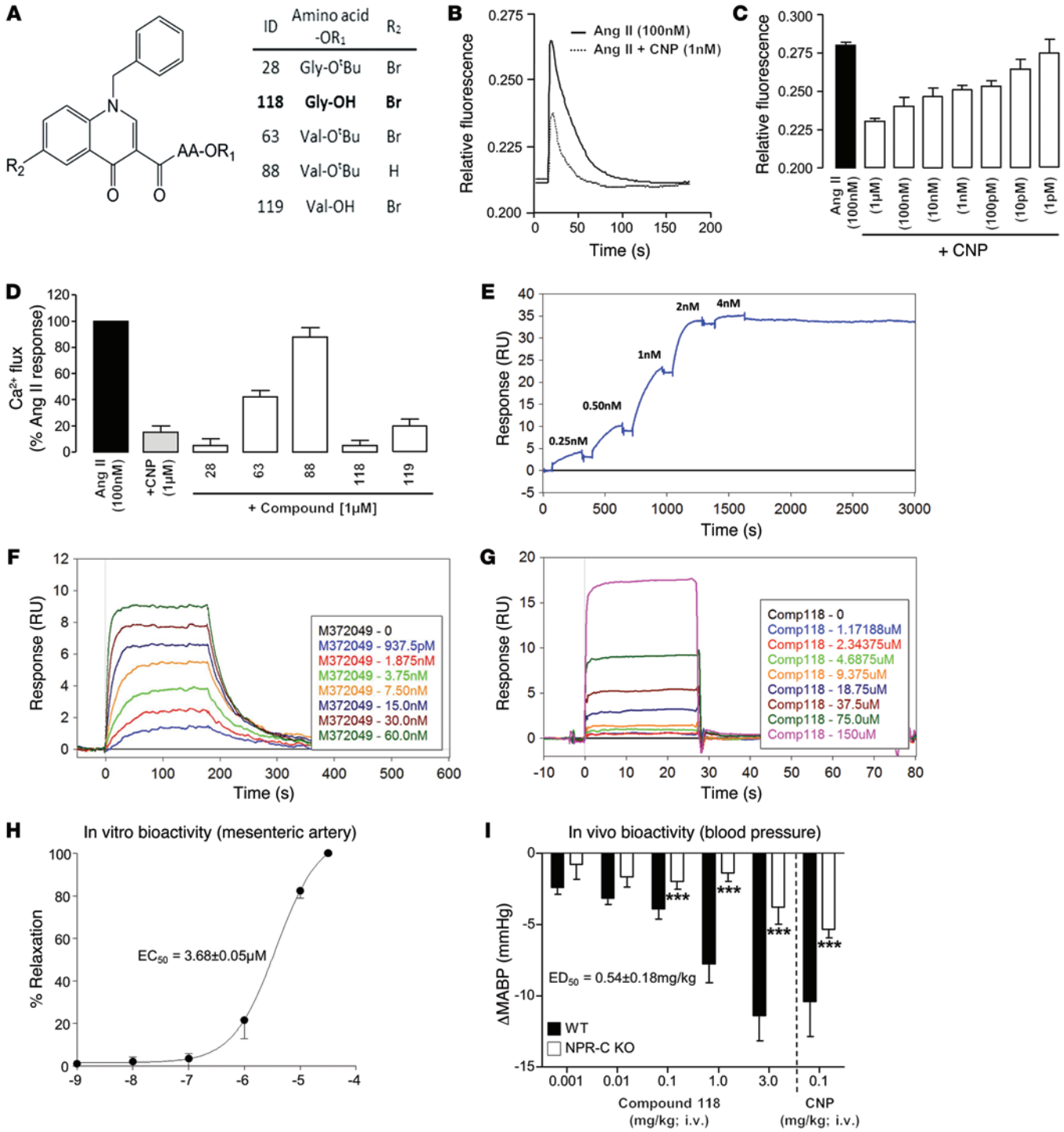

Figure 6. Chemical and biological characterization of NPR-C agonists. Structure of selected NPR-C agonists (**A**). Representative trace showing inhibition of the Ca^{2+} flux in response to angiotensin II (Ang II; 100 nM) by CNP in primary mesenteric artery smooth muscle cells using a FLIPR-based assay (**B** and **C**). Structure-activity relationship (SAR) for selected NPR-C agonist series using an identical cell-based assay (**D**). SPR spectroscopic analysis of the interaction of CNP (0.25–4 nM) (**E**), M372049 (1–60 nM) (**F**), and compound 118 (1–150 μM) (**G**) with human NPR-C (representative of 3 separate experiments). Vasorelaxant activity of lead NPR-C agonist, compound 118, in isolated mesenteric arteries (**H**), and the hypotensive effect of compound 118 in WT and NPR-C KO mice (**I**). Data are represented as the mean ± SEM. $n = 6$ for the in vitro and in vivo vascular reactivity studies and cell-based assays. ***$P < 0.001$, significantly different from WT littermates.

and J). Importantly, the accelerated atherogenesis in the ecCNP/ApoE dKO mice was not a result of altered plasma lipid profile or circulating cell numbers/subpopulations, since these parameters were not significantly different between the 2 genotypes (Supplemental Tables 4 and 5). No sex difference in atheroma progression was apparent (data are a composite of observations from male and female mice), and the enhanced plaque formation was not simply a consequence of hypertension, since both male ecCNP KO and

ecCNP/ApoE dKO mice were normotensive and female ecCNP KO and ecCNP/ApoE dKO mice had a commensurate higher MABP (Supplemental Table 6).

Unexpectedly, the ecCNP/ApoE dKO mice also developed aneurysms (Figure 5, A–D). This phenomenon was only observed in male mice, where approximately 50% (4/9) developed either aortic arch or abdominal aneurysms; since the male ecCNP KO mice did not exhibit a hypertensive phenotype, this effect is not pressure related. The morphological changes in the aortic wall were characterized by wall thinning (medial degeneration) and dilatation (aortic arch) and complete disruption of the internal elastic laminae (abdominal aorta), resulting in protrusion of the atheroma into the adventitia.

The effect of novel, small-molecule NPR-C agonists on vascular reactivity and blood pressure. Consistent with this multimodal cytoprotective profile of CNP in the vasculature, we proceeded to develop small-molecule NPR-C agonists based on the premise that activation of NPR-C would recapitulate the beneficial bioactivity of CNP. The lead molecules (design and synthesis of which will be described elsewhere), exemplified by compound 118 and related structures (Figure 6A), were discovered as a result of a systematic design program that identified key binding features of the natural ligand CNP and the peptide antagonist M372049 ascertained from the published crystal structure of NPR-C (47). In silico screening of virtual compound libraries was employed to select compounds with optimal predicted binding characteristics and drug-like properties; these were synthesized in house, and rapid evaluation of the potency of these molecules was assessed using a cell-based screening assay (Figure 6, B–D). The *tert*-butyl glycine ester (compound 28) and its corresponding acid (compound 118) showed potent activity. Amino acids with sterically bulky side chains such as valine (e.g., compounds 63 and 119; Figure 6A) showed lower activity. The bromine atom contributed to activity, and removal, as in compound 88, also diminished potency. Surface plasmon resonance (SPR) spectroscopy was used to confirm binding of endogenous ligand CNP, the selective receptor antagonist M372049, and compound 118 to human NPR-C (Figure 6, E–G). The physicochemical properties of 118 fall within general guidelines for drug likeness (48) and also have good in vitro and in vivo potency (Figure 6, H and I). For example, 118 causes relaxation of isolated mesenteric resistance arteries with an EC_{50} value of approximately 3 μM (Figure 6H), an effect blocked by NPR-C antagonism (Supplemental Figure 1L). Moreover, 118 causes dose-dependent reductions in blood pressure in anesthetized WT mice (ED_{50} < 1 mg/kg), which is significantly blunted in NPR-C KO animals (Figure 6I), demonstrating receptor selectivity.

Discussion

Endothelium-derived NO and PGI_2 are recognized as playing vascular homeostatic roles (1, 5, 6). Herein, using complementary genetic and pharmacological approaches, we provide evidence that endothelium-derived CNP represents an additional physiological regulator of vascular reactivity and integrity, governing smooth muscle tone, systemic blood pressure, and the activation of circulating leukocytes and platelets. This role appears equivalent in prominence to that of PGI_2 and NO, with a comparable diverse functional remit. In accord, disruption of CNP signaling precipitates endothelial dysfunction and hypertension, augments inflammatory cell and platelet activation, and accelerates the development of atherogenesis and aneurysm. Furthermore, we establish NPR-C as the cognate receptor that conveys the vasoprotective bioactivity of CNP and describe the design and development of small molecule NPR-C agonists that recapitulate the beneficial actions of CNP signaling in the vasculature.

This newly defined blood pressure regulatory role of endothelium-derived CNP, and specifically recognition of the involvement of NPR-C, provides a mechanism to explain our recent GWAS that identified and validated association of the NPR-C (*Npr3*) gene locus with blood pressure and adverse cardiovascular outcomes (49). Furthermore, our data explain other reported genetic associations linking the CNP (*Nppc*), NPR-C (*Npr3*), and *furin* (a proprotein convertase important in the processing of proCNP; ref. 50) loci to hypertension (49, 51–53). However, our findings are consistent with a dual capacity of NPR-C to act as a clearance receptor and a positive signaling mechanism responsive to endothelial CNP. The blood pressure difference between male NPR-C KO mice (7 mmHg lower than WT) and female NPR-C KO mice (7 mmHg higher than WT) is equivalent to the hypertension observed in female ecCNP KO mice (14 mmHg higher than WT), implying that deletion of NPR-C causes a small reduction in blood pressure in both sexes (consistent with a clearance function; ref. 26), which is counterbalanced by the loss of CNP/NPR-C signaling in females, resulting in an overall hypertensive phenotype. It remains to be elucidated whether individual receptors can both clear and signal or whether there are subpopulations that possess one or the other function. This differential activity might be cell-type dependent; for example, NPR-C expressed on endothelial cells would be more suited to clearing natriuretic peptides from the circulation, while NPR-C expressed on vascular smooth muscle cells may be configured to signal in response to endothelial CNP. Reports suggest that multiple NPR-C proteins exist with varying molecular weights and susceptibility to internalization (54), giving rise to the possibility that splice variants or posttranslational modification may influence function (i.e., clearance versus signaling). Further investigation is required to delineate whether polymorphisms within the *Npr3* gene functionally alter clearance, signaling, or both.

The current study also reveals a sex difference in the consequences of endothelial deletion of CNP on blood pressure control. This observation parallels data gleaned from our previous work utilizing mice doubly deficient in eNOS and COX-1 (9), and explains the mechanism by which females maintain normal blood pressure (i.e., via CNP release), whereas males are more reliant on endothelium-derived NO; such a sex difference has been suggested to underpin, in part, the lower incidence of cardiovascular disease in premenopausal women compared with age-matched male counterparts (8, 10). Whether a sex difference in CNP/NPR-C signaling is apparent in the human vasculature remains to be determined. This study identified a functional CNP/NPR-C signaling pathway in isolated human resistance arteries (i.e., equivalent vasorelaxant responses to CNP) in males and females, and our GWAS linking NPR-C genotype with hypertension (49) did not reveal a sex disparity. Such observations intimate that, in humans, both sexes signal via NPR-C to maintain blood pressure. However, the propensity of female sex

hormones to maintain higher natriuretic peptide levels (55) suggests that women, akin to mice, may place a greater reliance on endothelial CNP to regulate vascular homeostasis.

In addition to the maintenance of vascular dynamics and blood pressure, our data reveal that endothelium-derived CNP plays a role in preserving the integrity of the blood vessel wall; this is manifested in the ecCNP KO mouse as accelerated atherogenesis and aneurysm. This structural role for CNP is likely to stem from both direct and indirect salutary actions. The functional capacity of endothelium-derived CNP, delineated herein, in regulating vessel tone and the reactivity of leukocytes and platelets coupled to the peptide's ability to augment endothelial cell growth while inhibiting vascular smooth muscle cell proliferation (56) will undoubtedly contribute to offsetting the development of atherosclerotic lesions. However, a further direct effect on the blood vessel wall is likely. One common mechanism underpinning the development of atherosclerosis and aneurysm is the activation of MMPs, particularly MMP-2 and MMP-9 (57–59). This may be a key point of intervention of endothelium-derived CNP, since in chondrocytes, CNP overexpression reverses achondroplasia by reducing the activity and release of several MMPs, including both MMP-2 and MMP-9 (60), and CNP regulates the MMP/tissue inhibitors of metalloproteinases (TIMP) ratio to ameliorate renal fibrosis following ureteral obstruction (61). Our work might therefore explain the beneficial activity of neutral endopeptidase inhibitors, which prevent the endogenous breakdown of CNP (and other natriuretic peptides), in experimental models of atherosclerosis (62). This thesis is supported by observations in diseased human coronary arteries that expression of CNP is inversely correlated with severity of the lesion (63) and that CNP is a particularly potent inhibitor of oxidized LDL–stimulated vascular smooth muscle migration and mitogenesis, an integral component of complex lesion formation (64–66). Moreover, in many experimental models, pressor agents such as Angiotensin II are necessary to trigger the formation of aneurysm (67); ecCNP KO mice may offer a cleaner model with which to study this vascular disorder and shed light on the sex bias apparent in humans (68).

The identification of small-molecule agonists at NPR-C represents an excellent starting point for the development of drugs likely to exert multiple, beneficial effects in the cardiovascular system, although it remains to be established whether such compounds would recapitulate all of the cytoprotective functions of endothelium-derived CNP identified in this study. Regardless, these molecules confirm the "druggable" nature of NPR-C and have wider implications for the rationale design and development of small-molecule agonists targeted to large (in this case dimeric) GPCRs with endogenous peptide ligands, which has proven difficult to date (69–71). With respect to NPR-C, the lead molecules we have identified (particularly those that exhibit high affinity/slow dissociation) not only possess the potential to exert the plethora of vasoprotective effects verified above, but should also slow the removal of endogenous natriuretic peptides from the circulation by effectively competing for the "clearance" function of NPR-C (a mechanism for removal of natriuretic peptides from the circulation) (27); thus, the cardioprotective actions of endogenous natriuretic peptides will also be enhanced. Moreover, the vasorelaxant and hypotensive actions of lead NPR-C agonists are observed in males and females, indicating that the NPR-C signaling pathway is amenable to pharmacological manipulation in both sexes. As such, NPR-C agonists have potential as disease-modifying therapeutics for hypertension and other cardiovascular disorders.

Methods

Generation of an ecCNP KO mouse

This was achieved using a targeting vector constructed with 2 LoxP sites flanking the entire peptide coding region for CNP in exons 1 and 2 (Figure 1A). *Nppc*$^{fl/fl}$ animals, which had been backcrossed at least 10 times to a C57BL/6J background, were crossed with a mouse in which expression of Cre recombinase is driven by an endothelial-specific promoter/enhancer associated with the angiopoietin *Tie*^{2} receptor (72). Heterozygous animals at the *Nppc* locus that expressed the *Tie*^{2} transgene (*Tie*^{2}*-Cre Nppc*$^{+/fl}$) were used as breeding pairs to generate ecCNP KO and corresponding WT (*Tie*^{2}*-Cre Nppc*$^{+/+}$) littermate controls (Figure 1B). Offspring were produced according to Mendelian inheritance laws, and ecCNP KO mice gained weight at an equivalent rate to that of WT littermates, suggesting loss of endothelial CNP does not have any overt effect on development in utero or postpartum (data not shown).

In some studies, *Tie*^{2}*-Cre Nppc*$^{fl/fl}$ mice were crossed with *Apoe* KO mice (both C57BL/K6 background), and the *Tie*^{2}*-Cre Nppc*$^{+/fl}$ *Apoe*$^{+/-}$ offspring recrossed to obtain *Tie*^{2}*-Cre Nppc*$^{+/fl}$ *Apoe* KO animals. These were used as breeding pairs to generate *Tie*^{2}*-Cre Nppc*$^{+/+}$ *Apoe* KO (WT/Apoe KO) and *Tie*^{2}*-Cre Nppc*$^{fl/fl}$ *Apoe* KO (ecCNP/ApoE dKO) mice. From 5 weeks of age, animals were fed a high-fat (21% fat, 0.15% cholesterol; Lillico Biotechnology) Western style diet for 12 weeks.

Genotyping and qPCR analysis

Genomic DNA was prepared from ear biopsies for analysis by PCR using standard cycling parameters. The floxed allele was detected using the following primers: 5′-CCTTTATGCCAAGAGAACTTCCAGGAGG-3′ and 5′-TCCTTCCTGACTTCCTTCTGCTCTCTATCC-3′. These flank the second loxP site (Figure 1A), amplifying 842-bp (WT) and 956-bp (floxed) products. The primers used for the detection of the Tie^2-Cre transgene were 5′-CCTGTGCTCAGACAGAAATGAG-3′ and 5′-CGCATAACCAGTGAAACAGCATTGC-3′ (550 bp).

Total RNA was extracted (QIAGEN RNeasy Mini Kit) from endothelial cells, lung, liver, and kidney of ecCNP WT and KO animals to confirm selective deletion of CNP from the endothelium. Pulmonary microvascular endothelial cells were isolated as we described previously (56). 1 μg RNA was converted to cDNA using the QIAGEN Quantitect Reverse Transcription Kit (QIAGEN). Quantitative real-time PCR was performed using the Quantitect SYBR green kit (QIAGEN) with primers designed to detect CNP exon 2 (10 μM; 5′-CTGCACTAACATCCCAGACC-3′ and 5′-CTGGTGGCAATCAGAAAAAG-3′). Results were analyzed using the ABI PRISM 7900HT software package SDS 2.1 (Advanced Biotechnologies Ltd). Relative *Cnp* mRNA expression was determined using the $2^{-\Delta\Delta Ct}$ method. mRNA levels were normalized to 18S (internal control) for each sample, and gene expression was quantified as a fold change relative to ecCNP WT levels.

To determine CNP expression in specific circulating cell populations, 50 μl of whole blood diluted 1:1 with HEPES buffer was incubated with antibodies selective for mouse neutrophils (GR-1 FITC;

1:2500; clone RB6-8C5; eBioscience), monocytes (CD115 APC; 1:400; clone AFS98; eBioscience), T cells (CD3e PE Cy7; 1:100; clone 145-2C11; eBioscience) and B cells (CD19 Br Viol; 1:100; clone 6D5; BioLegend) for 30 minutes and cell populations sorted (ARIA II; BD). Total RNA was isolated from each cell type, and 200 ng of RNA was reverse transcribed and subjected to PCR analysis using the same primers and PCR conditions as above.

In vitro functional assessment of vessel reactivity

Murine arteries. The vascular reactivity of mouse thoracic aortic and mesenteric arterial vascular ring preparations was determined using classical tissue bath pharmacology, as we have described previously (9).

Human resistance arteries. Resistance arteries (200–500 μm) were isolated from omental fat obtained from patients (14 subjects, 6 female, mean age 4.4 ± 0.7 years) undergoing nonurgent, nonseptic abdominal surgery. The reactivity of arterial ring segments (2 mm long) was studied as described for the murine mesenteric arteries (above).

Radiotelemetric recording of hemodynamics and HRV in vivo

Blood pressure was recorded in conscious, freely moving mice using radiotelemetric transmitters (TA11PA-C10; Data Sciences International) implanted into the aortic arch. After 10 days recovery, the blood pressure was recorded for 24 hours in mice left undisturbed and maintained on a 12-hour light/12-hour dark cycle. Data were acquired for 2 minutes every 15 minutes, and the average values for MABP were calculated for every time point (Dataquest Art Acquisition System). HRV was analyzed in both frequency and time domains using standard HRV parameters (73) using the HRV extension module of Chart 4.0 (ADInstruments).

Leukocyte and platelet reactivity

Leukocyte recruitment was assessed in mesenteric postcapillary venules, as we have described previously (74).

Impedance aggregometry (Multiplate Dynabyte) was used to measure platelet reactivity in whole blood immediately after collection. 175 μl citrated blood diluted 1:1 vol/vol with 0.9% NaCl + 0.025 mmol/l $CaCl_2$ was equilibrated in the test cuvette for 3 minutes prior to the addition of collagen (3 and 10 μg/ml; Lab-Medics) or the thrombin receptor agonist PAR4-AP (300 μM; Sigma-Aldrich). Aggregation was monitored for 6 minutes and expressed as area under the curve.

Experimental peritonitis

Peritonitis was induced by subcutaneous injection of 300 ng TNF-α (Peprotech). After 4 hours, a peritoneal lavage was performed with 4 ml PBS, and the total leukocyte count in the lavage fluid was determined using a hemocytometer. In order to determine the cell types in the lavage fluid, 5×10^5 cells were incubated with antibodies selective for mouse neutrophils (GR-1 FITC; 20 ng; eBioscience) and inflammatory macrophages (double positive for GR-1 FITC and F4/80;125 ng; eBioscience) for 30 minutes prior to analysis on a flow cytometer (FACScalibur; BD). Data were collected from 10,000 events, and the total number of neutrophils and inflammatory macrophages in the lavage fluid was calculated using the percentage of positive cells measured in the flow cytometry sample.

An MPO assay was performed as second index of neutrophil accumulation. Mesenteric tissue was homogenized with 1 ml 0.5% hexadecyltrimethylammonium bromide (HTAB) in PBS (Sigma-Aldrich) using a bead homogenizer for 30 s at 2,000 *g*. Samples were then centrifuged for 5 minutes at 10,000 *g* and the supernatant removed for use in the assay. Mesenteric samples were diluted 1:2 in HTAB for analysis. 20 μl of standard (MPO 0.03 U/ml–1 U/ml; Sigma-Aldrich) and samples (duplicate) were added to a 96-well plate. 160 μl tetramethylbenzidine was added to each well, followed by 20 μl H_2O_2 (Sigma-Aldrich) and incubated for 5 minutes at room temperature (protected from light). The absorbance was read on a spectrophotometer at 620 nm. The protein content of each sample was determined using a Pierce BCA protein assay (Thermo Scientific) performed according to the manufacturer's instructions.

Flow cytometry

Whole blood was subjected to flow cytometric analysis to assess platelet P-selectin expression and platelet-leukocyte interactions. For P-selectin expression, 5 μl of citrated blood diluted 1:10 with HEPES buffer (composition: 150 mM NaCl, 5 mM KCl, 1 mM $MgSO_4$, 10 mM HEPES) was incubated with anti-mouse CD41-PE (glycoprotein IIb/IIIa; 1:200; clone eBioMWreg30; eBioscience) and anti-mouse CD62P-FITC (P-selectin; 1:200; clone RB40.34; BD Biosciences) for 30 minutes prior to analysis (FACScalibur; BD). The results are expressed as the percentage of platelets (CD41-positive cells) expressing the adhesion molecule P-selectin. The number of circulating platelet-leukocyte aggregates was determined by staining 50 μl blood (diluted 1:1 with HEPES buffer) with anti-mouse CD45-FITC (leukocyte common antigen; 1:200; clone 30-F11; eBioscience) and anti-mouse CD41-PE for 30 minutes prior to the addition of red blood cell lysis buffer (BD Biosciences). The results were expressed as the percentage of double-positive cells within the leukocyte population.

Characterization of atherosclerotic lesions

Animals were perfused with saline via the left ventricle, followed by 4% formaldehyde in aqueous buffered solution at physiological pressure to fix the vascular tree. The entire aorta was removed and opened longitudinally from the aortic root to the iliac bifurcation. Atherosclerotic lesions were stained with oil red O, as previously described (75). Images of en face staining were captured using a digital camera (Nikon D70), and the total area covered by plaque was quantified using Image Pro software. Brachiocephalic arteries from the same mice were embedded in paraffin wax, sectioned, and stained with H&E, anti–smooth muscle actin (1:400; clone 1A4; Sigma-Aldrich), and anti-Mac2 (1:6000; clone M3/38; Cedarlane). The intima-media thickness ratio and plaque size were analyzed using Axiovision 4.8.2 software. Cross sections of the aneurysms were stained with Elastic Van Gieson and anti–smooth muscle actin. Fasting plasma lipid levels were measured using a commercially available kit (Abcam).

Plasma CNP measurement

Plasma CNP was extracted (C18 columns) and measured using a commercially available ELISA kit (Phoenix Pharmaceuticals).

NPR-C agonist screening assays

Ca^{2+} flux in rat mesenteric vascular smooth muscle cells in response to angiotensin II. Measurements of Ca^{2+} flux in response to angiotensin II were conducted using a fluorescent imaging plate reader (FLIPR; Molecular Devices). Mesenteric artery smooth muscle cells isolated by collagenase digestion were plated at a density of 10,000 cells/well into black, clear-bottomed 96-well plates in DMEM supplemented

with penicillin (100 U/ml), streptomycin (100 μg/ml), L-glutamine (2 mM), and 10% heat inactivated New Zealand fetal calf serum. 24 hours later the cells were incubated with Fluo-3-AM (4 μM) for 60 minutes at 37°C. Once dye loaded, the cells were washed thoroughly with the proprietary assay buffer to remove any unincorporated dye. The cells were then incubated with NPR-C agonists, CNP, or vehicle (DMSO) and placed into the FLIPR. After 15 minutes, angiotensin II (100 nM) was automatically dispensed into each well and the fluorescence signal followed for 5 minutes. Potency was determined by comparison of the peak fluorescence in each test well (run in triplicate) with that of the control (angiotensin II alone). Background fluorescence (assay buffer only) was subtracted from all values.

SPR spectroscopy. All SPR analysis was performed on a BIAcore T200 system using series S CM5 sensor chips. Data processing and analysis were performed using BIAevaluation software and Scrubber2. All sensorgrams were double referenced by subtracting the response on a reference flow cell and a blank sample. Human NPR-C (OriGene) was covalently attached to a CM5 chip via amine coupling. A surface density of 2700 RU (~3.24 ng NPR-C protein) was used for measurements with natriuretic peptides and the NPR-C antagonist M372049, and a density of 5200 RU (~6.24 ng NPR-C protein) for measurements with compound 118. Sequential injections of CNP (0.25–4 nM) were performed at a flow rate of 30 μl/min (240 s for each), followed by a dissociation time of 3600 s. Binding site saturation was observed, and the surface was regenerated by 2 injections of 1 M NaCl (200 s each). Binding of M372049 (0.94–60 nM) and compound 118 (1.17–150 μM) was analyzed by sequential injections (120 s for M372049, 30 s for compound 118) followed by undisturbed dissociation (600 s for M372049, 30s for compound 118), during which curves returned to baseline. Kinetic parameters were calculated assuming a simple 1:1 (Langmuir) binding.

Statistics

For vascular reactivity studies, curves were fitted to the data using nonlinear regression (GraphPad software) and the –log (M) of each drug giving a half-maximal response (pEC_{50}) used to compare potency. Curves were analyzed using 2-way ANOVA with repeated measures. For in vivo studies, changes in MABP, leukocyte flux, and platelet reactivity were analyzed by 1-way ANOVA, with Bonferroni post-test where appropriate. Differences in atherosclerotic lesion size were analyzed by 2-tailed Student's *t* test. Normal distribution of data was confirmed by Shapiro-Wilk test. $P < 0.05$ was considered statistically significant. Results are expressed as mean ± SEM of *n* animals.

Study approval

All animal studies conformed to the UK Animals (Scientific Procedures) Act 1986 and were approved by the local ethics committee at the William Harvey Research Institute, Barts, and the London School of Medicine. Human vessels were collected from patients undergoing abdominal surgery after procuring written informed consent. Human studies were approved by the Ethics Committee of the Hospital Universitario Ramón y Cajal.

Acknowledgments

This work was supported by the Wellcome Trust (084449/Z/07/Z and 078496/Z/05/Z) and UCL Business PLC (PoC-12-007). This study forms part of the translational program of the National Institute for Health Research Biomedical Research Unit at Barts and The London School of Medicine and Dentistry.

Address correspondence to: Adrian J. Hobbs, William Harvey Research Institute, Barts, and The London School of Medicine and Dentistry, William Harvey Heart Centre, Queen Mary University of London, Charterhouse Square, London, UNK WC1E 6BQ. Phone: 44.0.207.882.5778; E-mail: a.j.hobbs@qmul.ac.uk.

Michela Simone's present address is: Department of Chemistry, School of Environmental and Life Sciences, University of Newcastle, Callaghan, New South Wales, Australia.

1. Vane JR, Anggard EE, Botting RM. Regulatory functions of the vascular endothelium. *N Engl J Med*. 1990;323(1):27–36.
2. Moncada S, Higgs A. The L-arginine-nitric oxide pathway. *N Engl J Med*. 1993;329(27):2002–2012.
3. Celermajer DS, Sorensen KE, Bull C, Robinson J, Deanfield JE. Endothelium-dependent dilation in the systemic arteries of asymptomatic subjects relates to coronary risk factors and their interaction. *J Am Coll Cardiol*. 1994;24(6):1468–1474.
4. Widlansky ME, Gokce N, Keaney JF, Keaney JF Jr, Vita JA. The clinical implications of endothelial dysfunction. *J Am Coll Cardiol*. 2003;42(7):1149–1160.
5. Ignarro LJ, Buga GM, Wood KS, Byrns RE, Chaudhuri G. Endothelium-derived relaxing factor produced and released from artery and vein is nitric oxide. *Proc Natl Acad Sci U S A*. 1987;84(24):9265–9269.
6. Palmer RM, Ferrige AG, Moncada S. Nitric oxide release accounts for the biological activity of endothelium-derived relaxing factor. *Nature*. 1987;327(6122):524–526.
7. Busse R, Edwards G, Feletou M, Fleming I, Vanhoutte PM, Weston AH. EDHF: bringing the concepts together. *Trends Pharmacol Sci*. 2002;23(8):374–380.
8. McCulloch AI, Randall MD. Sex differences in the relative contributions of nitric oxide and EDHF to agonist-stimulated endothelium-dependent relaxations in the rat isolated mesenteric arterial bed. *Br J Pharmacol*. 1998;123(8):1700–1706.
9. Scotland RS, et al. Investigation of vascular responses in endothelial nitric oxide synthase/cyclooxygenase-1 double-knockout mice: key role for endothelium-derived hyperpolarizing factor in the regulation of blood pressure in vivo. *Circulation*. 2005;111(6):796–803.
10. Barrett-Connor E. Sex differences in coronary heart disease. Why are women so superior? The 1995 Ancel Keys Lecture. *Circulation*. 1997;95(1):252–264.
11. de Bold AJ. Atrial natriuretic factor: a hormone produced by the heart. *Science*. 1985;230(4727):767–770.
12. Levin ER, Gardner DG, Samson WK. Natriuretic peptides. *N Engl J Med*. 1998;339(5):321–328.
13. Chusho H, et al. Dwarfism and early death in mice lacking C-type natriuretic peptide. *Proc Natl Acad Sci U S A*. 2001;98(7):4016–4021.
14. Komatsu Y, et al. Significance of C-type natriuretic peptide (CNP) in endochondral ossification: analysis of CNP knockout mice. *J Bone Miner Metab*. 2002;20(6):331–336.
15. Chen HH, Burnett JC, Burnett JC Jr. C-type natriuretic peptide: the endothelial component of the natriuretic peptide system. *J Cardiovasc Pharmacol*. 1998;32(suppl 3):S22–S28.
16. Ahluwalia A, Hobbs AJ. Endothelium-derived C-type natriuretic peptide: more than just a hyperpolarizing factor. *Trends Pharmacol Sci*. 2005;26(3):162–167.
17. Suga S, et al. Cytokine-induced C-type natriuretic peptide (CNP) secretion from vascular endothelial cells--evidence for CNP as a novel autocrine/paracrine regulator from endothelial cells. *Endocrinology*. 1993;133(6):3038–3041.
18. Stingo AJ, et al. Presence of C-type natriuretic peptide in cultured human endothelial cells and plasma. *Am J Physiol*. 1992;263(4 pt 2):H1318–H1321.
19. Sauer B, Henderson N. Site-specific DNA recom-

bination in mammalian cells by the Cre recombinase of bacteriophage P1. *Proc Natl Acad Sci U S A*. 1988;85(14):5166–5170.
20. Mitchell JA, De NG, Warner TD, Vane JR. Different patterns of release of endothelium-derived relaxing factor and prostacyclin. *Br J Pharmacol*. 1992;105(2):485–489.
21. Morley D, Keefer LK. Nitric oxide/nucleophile complexes: a unique class of nitric oxide-based vasodilators. *J Cardiovasc Pharmacol*. 1993;22(suppl 7):S3–S9.
22. Lahiri MK, Kannankeril PJ, Goldberger JJ. Assessment of autonomic function in cardiovascular disease: physiological basis and prognostic implications. *J Am Coll Cardiol*. 2008;51(18):1725–1733.
23. Potter LR, Yoder AR, Flora DR, Antos LK, Dickey DM. Natriuretic peptides: their structures, receptors, physiologic functions and therapeutic applications. *Handb Exp Pharmacol*. 2009;(191):341–366.
24. Chauhan SD, Nilsson H, Ahluwalia A, Hobbs AJ. Release of C-type natriuretic peptide accounts for the biological activity of endothelium-derived hyperpolarizing factor. *Proc Natl Acad Sci U S A*. 2003;100(3):1426–1431.
25. Villar IC, et al. Definitive role for natriuretic peptide receptor-C in mediating the vasorelaxant activity of C-type natriuretic peptide and endothelium-derived hyperpolarising factor. *Cardiovasc Res*. 2007;74(3):515–525.
26. Matsukawa N, et al. The natriuretic peptide clearance receptor locally modulates the physiological effects of the natriuretic peptide system. *Proc Natl Acad Sci U S A*. 1999;96(13):7403–7408.
27. Maack T, et al. Physiological role of silent receptors of atrial natriuretic factor. *Science*. 1987;238(4827):675–678.
28. Tamura N, Doolittle LK, Hammer RE, Shelton JM, Richardson JA, Garbers DL. Critical roles of the guanylyl cyclase B receptor in endochondral ossification and development of female reproductive organs. *Proc Natl Acad Sci U S A*. 2004;101(49):17300–17305.
29. Nakamura M, Arakawa N, Yoshida H, Makita S, Hiramori K. Vasodilatory effects of C-type natriuretic peptide on forearm resistance vessels are distinct from those of atrial natriuretic peptide in chronic heart failure. *Circulation*. 1994;90(3):1210–1214.
30. Honing ML, Smits P, Morrison PJ, Burnett JC, Burnett JC Jr, Rabelink TJ. C-type natriuretic peptide-induced vasodilation is dependent on hyperpolarization in human forearm resistance vessels. *Hypertension*. 2001;37(4):1179–1183.
31. Igaki T, et al. C-type natriuretic peptide in chronic renal failure and its action in humans. *Kidney Int Suppl*. 1996;55:S144–S147.
32. Stingo AJ, Clavell AL, Aarhus LL. Cardiovascular and renal actions of C-type natriuretic peptide. *Am J Physiol*. 1992;262(1 pt 2):H308–H312.
33. Clavell AL, Stingo AJ, Wei CM, Heublein DM, Burnett JC, Burnett JC Jr. C-type natriuretic peptide: a selective cardiovascular peptide. *Am J Physiol*. 1993;264(2 pt 2):R290–R295.
34. Seymour AA, Mathers PD, Abboa-Offei BE, Asaad MM, Weber H. Renal and depressor activity of C-natriuretic peptide in conscious monkeys: effects of enzyme inhibitors. *J Cardiovasc Pharmacol*. 1996;28(3):397–401.
35. Trachte GJ. Depletion of natriuretic peptide C receptors eliminates inhibitory effects of C-type natriuretic peptide on evoked neurotransmitter efflux. *J Pharmacol Exp Ther*. 2000;294(1):210–215.
36. Rose RA, Giles WR. Natriuretic peptide C receptor signalling in the heart and vasculature. *J Physiol*. 2008;586(2):353–366.
37. Murthy KS, Teng BQ, Jin JG, Makhlouf GM. G protein-dependent activation of smooth muscle eNOS via natriuretic peptide clearance receptor. *Am J Physiol Cell Physiol*. 1998;275(6 pt 1):C1409–C1416.
38. Sciarretta S, et al. C2238 atrial natriuretic peptide molecular variant is associated with endothelial damage and dysfunction through natriuretic peptide receptor C signaling. *Circ Res*. 2013;112(10):1355–1364.
39. Li Y, Sarkar O, Brochu M, Anand-Srivastava MB. Natriuretic peptide receptor-C attenuates hypertension in spontaneously hypertensive rats: role of nitroxidative stress and Gi proteins. *Hypertension*. 2014;63(4):846–855.
40. Veale CA, et al. The discovery of non-basic atrial natriuretic peptide clearance receptor antagonists. Part 1. *Bioorg Med Chem Lett*. 2000;10(17):1949–1952.
41. Ley K, Laudanna C, Cybulsky MI, Nourshargh S. Getting to the site of inflammation: the leukocyte adhesion cascade updated. *Nat Rev Immunol*. 2007;7(9):678–689.
42. Michelson AD, et al. In vivo tracking of platelets: circulating degranulated platelets rapidly lose surface P-selectin but continue to circulate and function. *Proc Natl Acad Sci U S A*. 1996;93(21):11877–11882.
43. Furman MI, et al. Increased platelet reactivity and circulating monocyte-platelet aggregates in patients with stable coronary artery disease. *J Am Coll Cardiol*. 1998;31(2):352–358.
44. Mayadas TN, Johnson RC, Rayburn H, Hynes RO, Wagner DD. Leukocyte rolling and extravasation are severely compromised in P selectin-deficient mice. *Cell*. 1993;74(3):541–554.
45. Zhang SH, Reddick RL, Piedrahita JA, Maeda N. Spontaneous hypercholesterolemia and arterial lesions in mice lacking apolipoprotein E. *Science*. 1992;258(5081):468–471.
46. Plump AS, et al. Severe hypercholesterolemia and atherosclerosis in apolipoprotein E-deficient mice created by homologous recombination in ES cells. *Cell*. 1992;71(2):343–353.
47. He X, Chow D, Martick MM, Garcia KC. Allosteric activation of a spring-loaded natriuretic peptide receptor dimer by hormone. *Science*. 2001;293(5535):1657–1662.
48. Lipinski CA. Drug-like properties and the causes of poor solubility and poor permeability. *J Pharmacol Toxicol Methods*. 2000;44(3):235–249.
49. Ehret GB, et al. Genetic variants in novel pathways influence blood pressure and cardiovascular disease risk. *Nature*. 2011;478(7367):103–109.
50. Wu C, Wu F, Pan J, Morser J, Wu Q. Furin-mediated processing of Pro-C-type natriuretic peptide. *J Biol Chem*. 2003;278(28):25847–25852.
51. Ono K, Mannami T, Baba S, Tomoike H, Suga S, Iwai N. A single-nucleotide polymorphism in C-type natriuretic peptide gene may be associated with hypertension. *Hypertens Res*. 2002;25(5):727–730.
52. Pitzalis MV, et al. Allelic variants of natriuretic peptide receptor genes are associated with family history of hypertension and cardiovascular phenotype. *J Hypertens*. 2003;21(8):1491–1496.
53. Aoi N, et al. Variable number of tandem repeat of the 5'-flanking region of type-C human natriuretic peptide receptor gene influences blood pressure levels in obesity-associated hypertension. *Hypertens Res*. 2004;27(10):711–716.
54. Brown J, Zuo Z. Receptor proteins and biological effects of C-type natriuretic peptides in the renal glomerulus of the rat. *Am J Physiol*. 1994; 266(4 pt 2):R1383–R1394.
55. Lam CS, et al. Influence of sex and hormone status on circulating natriuretic peptides. *J Am Coll Cardiol*. 2011;58(6):618–626.
56. Khambata RS, Panayiotou CM, Hobbs AJ. Natriuretic peptide receptor-3 underpins the disparate regulation of endothelial and vascular smooth muscle cell proliferation by C-type natriuretic peptide. *Br J Pharmacol*. 2011;164(2b):584–597.
57. Newby AC. Metalloproteinase expression in monocytes and macrophages and its relationship to atherosclerotic plaque instability. *Arterioscler Thromb Vasc Biol*. 2008;28(12):2108–2114.
58. Thompson RW, et al. Production and localization of 92-kilodalton gelatinase in abdominal aortic aneurysms. An elastolytic metalloproteinase expressed by aneurysm-infiltrating macrophages. *J Clin Invest*. 1995;96(1):318–326.
59. Goodall S, Crowther M, Hemingway DM, Bell PR, Thompson MM. Ubiquitous elevation of matrix metalloproteinase-2 expression in the vasculature of patients with abdominal aneurysms. *Circulation*. 2001;104(3):304–309.
60. Krejci P, et al. Interaction of fibroblast growth factor and C-natriuretic peptide signaling in regulation of chondrocyte proliferation and extracellular matrix homeostasis. *J Cell Sci*. 2005;118(pt 21):5089–5100.
61. Hu P, Wang J, Zhao XQ, Hu B, Lu L, Qin YH. Overexpressed C-type natriuretic peptide serves as an early compensatory response to counteract extracellular matrix remodeling in unilateral ureteral obstruction rats. *Mol Biol Rep*. 2013;40(2):1429–1441.
62. Kugiyama K, Sugiyama S, Matsumura T, Ohta Y, Doi H, Yasue H. Suppression of atherosclerotic changes in cholesterol-fed rabbits treated with an oral inhibitor of neutral endopeptidase 24.11 (EC 3.4.24.11). *Arterioscler Thromb Vasc Biol*. 1996;16(8):1080–1087.
63. Casco VH, Veinot JP, Kuroski de Bold ML, Masters RG, Stevenson MM, de Bold AJ. Natriuretic peptide system gene expression in human coronary arteries. *J Histochem Cytochem*. 2002;50(6):799–809.
64. Kohno M, et al. Effect of natriuretic peptide family on the oxidized LDL-induced migration of human coronary artery smooth muscle cells. *Circ Res*. 1997;81(4):585–590.
65. Furuya M, et al. C-type natriuretic peptide is a growth inhibitor of rat vascular smooth muscle cells. *Biochem Biophys Res Commun*. 1991;177(3):927–931.
66. Cahill PA, Hassid A. Clearance receptor-binding atrial natriuretic peptides inhibit mitogenesis and proliferation of rat aortic smooth muscle cells. *Biochem Biophys Res Commun*. 1991;179(3):1606–1613.

67. Daugherty A, Cassis LA. Mouse models of abdominal aortic aneurysms. *Arterioscler Thromb Vasc Biol*. 2004;24(3):429–434.
68. Pleumeekers HJ, et al. Aneurysms of the abdominal aorta in older adults. The Rotterdam Study. *Am J Epidemiol*. 1995;142(12):1291–1299.
69. Blakeney JS, Reid RC, Le GT, Fairlie DP. Nonpeptidic ligands for peptide-activated G protein-coupled receptors. *Chem Rev*. 2007;107(7):2960–3041.
70. Mason JS, Bortolato A, Congreve M, Marshall FH. New insights from structural biology into the druggability of G protein-coupled receptors. *Trends Pharmacol Sci*. 2012;33(5):249–260.
71. Cheng AC, et al. Structure-based maximal affinity model predicts small-molecule druggability. *Nat Biotech*. 2007;25(1):71–75.
72. Kisanuki YY, Hammer RE, Miyazaki J, Williams SC, Richardson JA, Yanagisawa M. Tie2-Cre transgenic mice: a new model for endothelial cell-lineage analysis in vivo. *Dev Biol*. 2001;230(2):230–242.
73. Zuberi Z, Birnbaumer L, Tinker A. The role of inhibitory heterotrimeric G proteins in the control of in vivo heart rate dynamics. *Am J Physiol Regul Integr Comp Physiol*. 2008;295(6):R1822–R1830.
74. Ahluwalia A, et al. Antiinflammatory activity of soluble guanylate cyclase: cGMP-dependent down-regulation of P-selectin expression and leukocyte recruitment. *Proc Natl Acad Sci U S A*. 2004;101(5):1386–1391.
75. Laxton RC, et al. A role of matrix metalloproteinase-8 in atherosclerosis. *Circ Res*. 2009;105(9):921–929.